Scientia Iranica B (2020) 27(5), 2443–2450

Sharif University of Technology
Scientia Iranica
Transactions B: Mechanical Engineering
http://scientiairanica.sharif.edu

Effect of welding parameters on dissimilar pulsed laser joint between nickel-based alloy Hastelloy X and austenitic stainless steel AISI 304L

F. Vakili Tahami[a,*], E. Safari[b], and H. Halimi Khosroshahi[a]

a. *Department of Mechanical Engineering, University of Tabriz, Tabriz, P.O. Box 51666-16471, Iran.*
b. *Faculty of Physics, University of Tabriz, Tabriz, P.O. Box 51666-16471, Iran.*

Received 1 December 2018; received in revised form 15 April 2019; accepted 15 July 2019

KEYWORDS
Hastelloy X;
Stainless steel;
Laser welding;
Scan electron microscope;
Nd-YAG laser;
Dissimilar welding.

Abstract. The present study aims to investigate the strength and microstructure of dissimilar weld joints composed of Hastelloy X, i.e., a nickel-based superalloy, and austenitic stainless steel 304L. Nd-YAG solid-state pulsed laser is used to perform welding between these two alloys. The effects of welding speed, laser power, and pulse width on the joint strength are studied by changing the values of the mentioned parameters. Then, the test samples were adopted to conduct uniaxial tensile tests at room temperature. The results obtained from the uniaxial tensile tests showed that the pulse width and laser beam power had maximum effects on the strength of the joint. Results also indicated that a dissimilar joint with the highest quality could be obtained by optimizing the welding power, beam pulse width, and welding speed. Given the selected parameters for laser welding, the tensile strength of the joint was equal to 95.5% of the weaker alloy strength (AISI 304L), which showed excellent quality of the weld. Furthermore, changes in the composition of the constituting elements of the joint were investigated using the Energy-Dispersive X-Ray Spectroscopy (EDS) tests and scanning electron microscope. The results of the EDS tests indicated that a change in the composition of the constituting elements in this zone occurred on a regular basis.

1. Introduction

Nickel-based superalloys and austenitic stainless steels enjoy various applications due to their high corrosion resistance and high temperature strength. Therefore, they are widely used in industries such as petrochemical, oil, and power plants [1–4]. To benefit from their advantages and, also, maintain a good balance in terms of material prices, dissimilar joining of these two alloys can be considered as an attractive option in designing and manufacturing the components of mechanical engineering.

One of the methods used for the permanent dissimilar joining of these two alloys is utilizing the various welding processes. To this end, a number of researchers have studied the welding of nickel-based superalloys and austenitic stainless steels [5–8]. Among different welding methods, laser beam welding is of considerable importance due to its centralized nature and very high thermal density. Laser beams can create narrow joints with high strength, small heat affected zone, and low residual stresses [9,10]. There can be a

*. *Corresponding author. Tel.: +98 41 33392463; Fax: +98 41 33354153*
E-mail address: f_vakili@tabrizu.ac.ir (F. Vakili Tahami)

doi: 10.24200/sci.2019.52221.2602

significant interaction between metal surfaces and solid state lasers, with beam delivery advantages. Hence, solid state lasers are among the most commonly used types of lasers used for material processing; Nd-YAG type lasers belong to this category [9,11].

Laser beams usage for material processing has a long history. The first laser application for welding purposes dates back to the mid-1960s [12,13]. At around the same time, the first attempts were made to weld dissimilar metals [14]. In recent years, with the developments of modern laser welding devices, great advances have been made in the field of laser welding of metals and even non-metals [15–18]. Mai and Spowage [19] studied steel-quartz, copper-steel, and copper-aluminum dissimilar laser welding and established strong joints for these three compounds using the Nd-YAG pulsed laser beam. They concluded that controlling the melting points of metals was an essential factor in the flawless process of welding dissimilar metals. Due to the centralized and limited nature of the laser beam, it is possible to control the heat distribution during the process, thus preventing the formation of brittle intermetallic phases during the welding process. Liu et al. [20,21] utilized Nd-YAG continuous laser beam for welding dissimilar plates of nickel-based alloy and alloyed steel. They investigated the effects of welding speed parameters, the protective gas flow rate, and non-focus distance. Their obtained results showed that high-quality deep-penetration laser welding could be achieved by optimizing welding parameters such as the welding speed and protective gas rate. Neves et al. [22] investigated end-to-end dissimilar joining of AISI 304 stainless steel and Inconel 600 using the pulsed Nd-YAG laser beam and established joints with maximum tensile strength equal to 90% of the base metal strength of AISI 304. Choobi et al. [23] studied clamping on residual stresses and distortions in butt-welded plates. Mortezaie and Shamanian [24] examined the dissimilar welding of Inconel 718 and austenitic stainless steel AISI 310S using the gas tungsten arc welding method with various fillers and concluded that the best filler to weld these two alloys, regarding the joint strength and corrosion resistance, is Inconel 625 filler. Ates et al. [25] developed an artificial neural network approach to predict the strength of welding joints. Manikandan et al. [26] examined the dissimilar Incoloy 800 and AISI 316L steel using 'gas tungsten arc welding' and 'shield metal arc welding' methods and established excellent joints with a strength higher than the weaker base metal strength (AISI 316L). Kumar and Sinha [27] studied the distribution of temperature fields in dissimilar welding of AISI 304L and St37 by using a 3D moving thermal source and obtained good agreement between finite element model and experimental results. Kumar and Sinha [28] examined the effect of Nd-YAG laser pulse width on the weld seam profile, penetration depth, and heat-affected zone for welding the austenitic stainless steel AISI 304L and carbon steel St37 and achieved joint strength higher than the weaker base alloy (St37) strength.

Review of the literature reveals that the dissimilar joining of Hastelloy X and AISI 304L has not been investigated thoroughly yet. Despite extensive studies on laser welding and microstructure of the laser joints, few studies have been conducted on the mechanical behavior of dissimilar laser welding of nickel-based superalloys and austenitic stainless steels and on the effect of welding parameters on the mentioned behavior. The significant novelties of this research comprise investigation of the effect of these three parameters (welding power, welding speed, and pulse width) on the dissimilar AISI 304L and Hastelloy X, determining joint strength based on the experimental tests in various conditions, and finding proper welding parameters. Both of these alloys are widely used in aerospace, power generating, petroleum industries, and chemical process components. Hastelloy enjoys properties superior to those of AISI 304L alloy and is among the first choices whose temperature level is very high. However, the former alloy is more expensive than the latter (more than ten times). To minimize the overall materials' price, there is a great tendency in the industry to use both alloys in manufacturing a single part like furnace nozzles, flame holders, and other combustion zone components including the section that sustains a higher temperature level (more than 500-600°C) in Hastelloy X and the section that undergoes a medium-level temperature in AISI 304L [29,30]. Typically, in these applications, permanent dissimilar joining of these two alloys is necessary. Joining these two sections with proper mechanical and microstructure properties is a significant concern in the related industries. Therefore, in this study, the performance of dissimilar Nd-YAG pulsed laser joint of the nickel-based superalloy Hastelloy X and 304L austenitic stainless steel is investigated by conducting the uniaxial tensile tests at room temperature and elemental composition of the joint.

2. Experimental procedures

Plates with a thickness of 1 mm were used for dissimilar welding. The plate's materials included 304L austenitic stainless steel and Hastelloy X nickel-based superalloy. Their chemical compositions based on weight percentage are given in Table 1. As shown in Table 1, for Hastelloy X, nickel is balanced and for AISI 304L alloy, iron is balanced.

The edges of the plates were prepared and cleaned prior to the welding process by using different grades of sandpaper sheets and acetone. Figure 1 presents the geometrical location of the plates relative to each other

Table 1. Compositions of nickel-based Hastelloy X and 304L stainless steel (wt.%).

Materials	Ni	Fe	Cr	Mo	Co	W	C	Mn	Si	S	P	B
Hastelloy X	Balance	18	22	9	1.5	0.6	0.10	≤ 1	≤ 1	—	—	≤ 0.008
AISI 304L	8.0–12.0	Balance	17.5–19.5	—	—	—	≤ 0.030	≤ 2.00	≤ 0.75	≤ 0.03	≤ 0.045	—

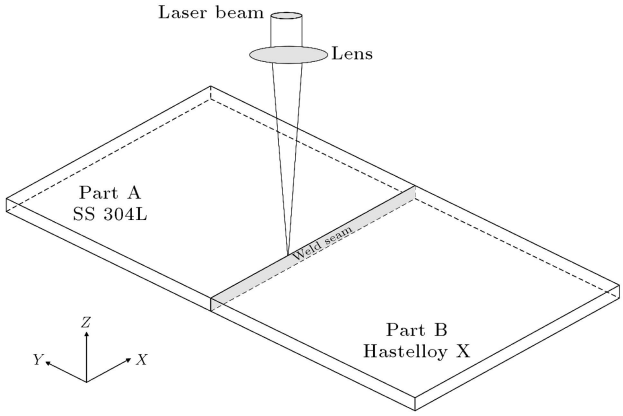

Figure 1. Setup of dissimilar butt welding of two alloys.

and also the method used to apply the laser beam. As shown in Figure 1, two pieces of plates are placed side by side (butt welding configuration) and are fixed to their places using a standard jig-fixture clamp.

The welding process is run using the Nd-YAG pulsed laser source model IQL-10 with the maximum average power of 400 W. A LpOphir power meter with maximum measurable power of 5000 W was used to measure the average laser beam power. The dissimilar welding of these two alloys is performed using the welding parameters given in Table 2. In all welds, argon shroud gas was delivered through a nozzle at a flow rate of 10 L/min. The distance between the focusing lens and the substrate surface and, also, laser beam frequency were kept constant at 2 mm and 20 Hz, respectively.

In pulsed lasers, the laser beam is composed of sequential pulses (Figure 2). The average beam power is equal to the sum of the energy of pulses per unit time (second), and the maximum pulse power is equal to the energy of a single pulse divided by the pulse width of the beam. The average beam power is measured by using a power meter, and the laser beam output is set to a desired value. Given that the frequency of the beam is kept constant at 20 Hz, the maximum power and the energy of each pulse can be calculated. The maximum power and pulse values are given in Table 2.

The spot-to-spot overlap is shown in Figure 3. If the diameter of the beam and welding speed are given, it is possible to calculate the overlapping percent of the pulses (Eq. (1)). Spot overlap percentages of different welding speeds are given in Table 2.

$$\frac{spot\ overlap}{100} = 1 - \left(\frac{welding\ speed}{spot\ diameter \times pulse\ rep\ rate} \right). \quad (1)$$

After welding, an electric discharge cutting machine is used to produce test samples in order to conduct

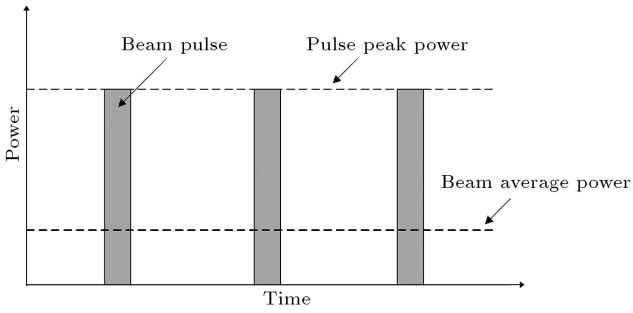

Figure 2. Pulsed laser beam.

Table 2. Parameters used in dissimilar welding of AISI 304L and Hastelloy X.

Sample no.	Average power (W)	Pulse width (ms)	Welding speed (mm/s)	Maximum pulse power (W)	Pulse energy (J)	Spot overlap (%)
1	200	5.5	5.84	1818	10	58.28
2	240	5.5	5.84	2182	12	58.28
3	275	5.5	5.84	2500	13.75	58.28
4	240	4.5	5.84	2667	12	58.28
5	240	6.5	5.84	1846	12	58.28
6	240	5.5	4.5	2182	12	67.86
7	240	5.5	6.67	2182	12	52.36

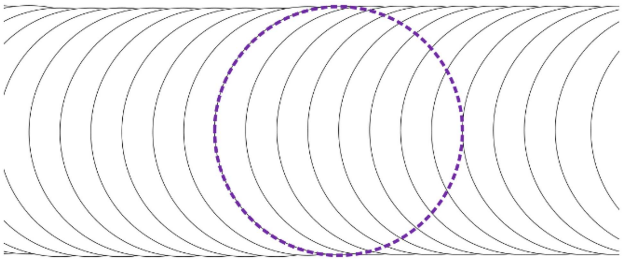

Figure 3. Laser beam pulses overlap.

uniaxial tensile tests. The drawing of the tensile test samples is shown in Figure 4(a), and an image of a test sample (before the test) is shown in Figure 4(b). As shown in Figure 4(b), the welding joints are in the middle of the samples and perpendicular to the direction of the tensile force.

As shown in Figure 4, two holes are considered at the two ends of the sample to apply the tensile force using the pin. This tensile test method makes the entire length of the parallel area out of the grips of the tensile test machine, and the extensometers can be easily attached to the sample. The samples are designed by analyzing the stress fields using finite element software, and the stress distribution of the parallel region is negligibly affected by the holes. The resulting samples are also employed in high-temperature and creep tests, which, for high-temperature testing that uses the pin to apply force, is more suitable than friction gripping methods.

The Energy-Dispersive X-Ray Spectroscopy (EDS) method was employed to investigate the change of the material composition and microstructure of the weldment using the Scanning Electron Microscope (SEM) model Tescan SEM5001 (Figure 5). A section of the weld seam, which is perpendicular to the welding direction, is produced from the welded sample,

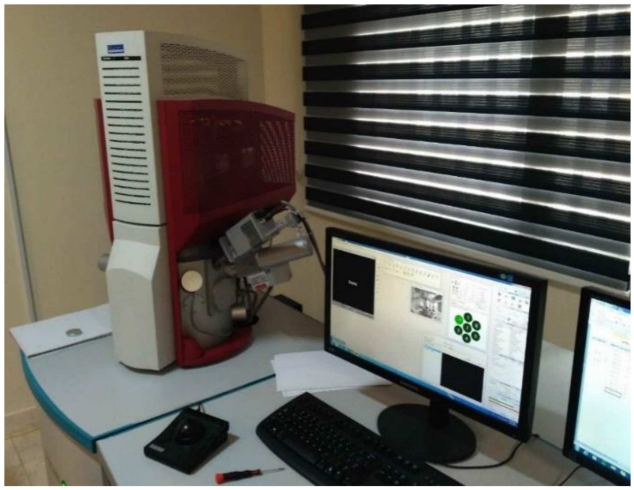

Figure 5. Scanning electron microscope model Tescan SEM5001.

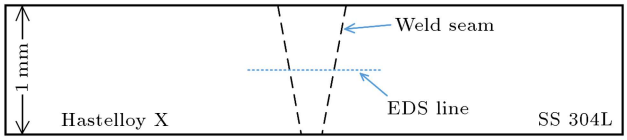

Figure 6. Weld seam examined by scan electron microscope.

as shown in Figure 6. After preparing the samples, the investigation was conducted via the scan electron microscope.

3. Results and discussion

For base alloys as well as welding samples, uniaxial tensile tests were carried out at room temperature. The results of the tensile tests for the base alloys and the following joints are shown in Table 3; their stress-

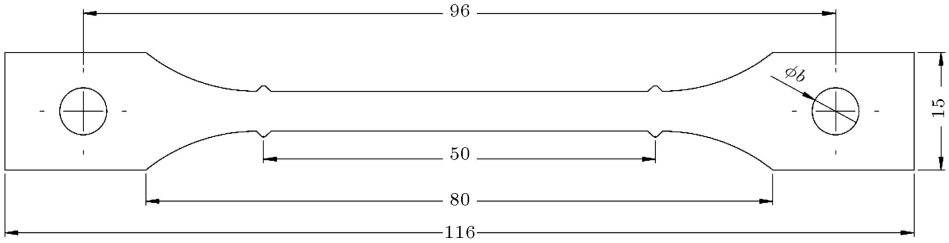

(a)

(b)

Figure 4. Uniaxial tensile sample.

Table 3. Results for the tensile tests at room and high temperatures.

Sample	Yield strength (MPa)	Ultimate strength at room temperature (MPa)	Ultimate strength/ ultimate strength of 304L (%)	Elongation (%)
304L base alloy	310.41	631.2	100	59.49
Hastelloy X base alloy	341.56	735.95	116.6	51.125
1	322.86	523.39	82.92	16.11
2	325.22	602.8	95.5	29.61
3	322.92	569.34	90.2	23.76
4	322.16	534	84.6	18.37
5	320.35	542.83	86	20.13
6	321.04	596.06	94.43	28.26
7	321.37	564.64	89.45	22.33

strain diagram at room temperature for the base alloys is shown in Figure 7. As shown in Table 3, at room temperature, the base alloy strength of 304L austenitic stainless steel and Hastelloy X nickel-based superalloy is 631.2 MPa and 735.95 MPa, respectively. Moreover, in column 4 of Table 3, the ratios of the ultimate strength of the samples to the final strength of the weaker base alloy (304L) are given in percentage.

3.1. Welding power and pulse width

In order to investigate the effect of laser beam power on the strength of the dissimilar joint, three different average powers, i.e., 200, 240, and 275 W, were employed. In all these cases, the welding speed, pulse width, and laser frequency were kept constant at 5.84 mm/s, 5.5 ms, and 20 Hz, respectively. The maximum laser pulse power depends on the average power, pulse width, and laser frequency. In constant pulse width (5.5 ms) and laser frequency (20 Hz), different average powers represent different maximum pulse powers: at average laser powers of 200, 240, and 275 W, the corresponding maximum pulse powers are 1818, 2182, and 2500 W, respectively. As listed in Table 3, at an average welding power of 200 W, the strength rates of the joint are 83%, 95.5%, and 90% of the weaker base alloy (SS304L) strength. In all these cases, rupture in the joint location occurred.

In order to investigate the effect of laser pulse width on the strength of the dissimilar joint, three different pulse widths of 4.5, 5.5, and 6.5 ms were used. In all these cases, the welding speed, average laser power, and laser frequency were kept constant at 5.84 mm/s, 240 W, and 20 Hz, respectively. At the constant average power (W) and laser frequency (20 Hz), different pulse widths represent different maximum pulse powers: For pulse widths of 4.5, 5.5, and 6.5 ms, the maximum pulse powers are 2667, 2182, and 1846 W, respectively. As shown in Table 3, at 4.5, 5.5, and, 6.5 ms pulse widths, the strength rates of the joint are 85%, 95.5%, and 86%, respectively, of the weaker base alloy (AISI 304L) strength. In all these cases, rupture in the joint location occurred.

Variations in the joint's ultimate strength with the welding power and pulse width (at a constant welding speed of 5.84 mm/s) are shown in Figure 8. As

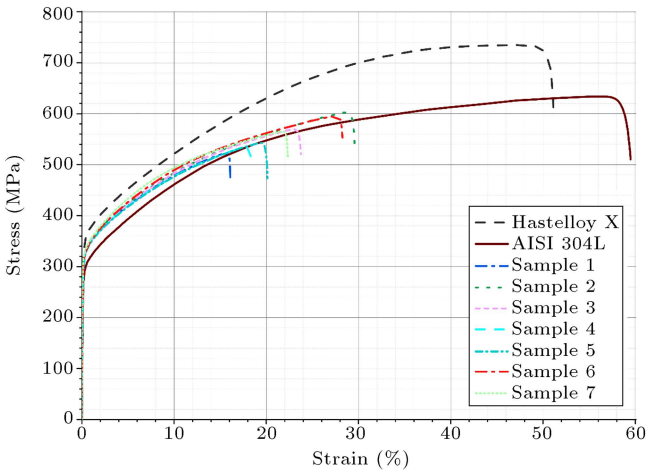

Figure 7. Stress-strain diagrams for the base alloys and samples.

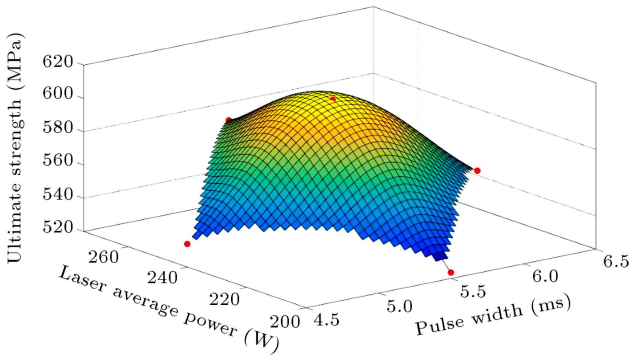

Figure 8. Variation of the joints' ultimate strength with welding power and pulse width.

observed, at constant pulse width and welding speed, by increasing the welding power, the joint strength increases and reaches its maximum value at 240 W and, then, the joint strength decreases. Further, at constant welding power and speed, by increasing the pulse width, the joint strength increases and reaches its maximum value and, then, the joint strength decreases. Moreover, the maximum strength is achieved at a welding power of 240 W and pulse width of 5.5 ms.

3.1.1. Welding speed

In order to investigate the effect of welding speed on the strength of the dissimilar joint, three different welding speeds were considered: 4.5, 5.84, and 6.67 mm/s. In all these cases, the pulse width, average laser power, and laser frequency were kept constant at 5.5 ms, 240 W, and 20 Hz, respectively. In addition, the distance between the focusing lens and the substrate surface was kept constant. Therefore, the laser beam spot size on the substrates top surface was constant and measured to be 700 μm. Changing the laser welding speed will change the spot-to-spot overlap percentage. At a constant spot size of 700 μm and pulse frequency of 20 Hz, the overlap percentage for welding speeds of 4.5, 5.84, and 6.67 mm/s can be calculated as 67.86%, 58.28%, and 52.36%, respectively. As seen in Table 3, at welding speeds of 4.5, 5.84, and 6.67 mm/s, the joint strength rates are 94.4%, 95.5%, and 89.5% of the weaker base alloy (AISI 304L) strength. In all these cases, rupture in the joint location occurred.

4. Microscope and SEM/EDS analysis

Weld appearance for the best joint (at a welding power of 240 W, pulse width of 5.5 ms, and welding speed of 5.84 mm/s) is shown in Figure 9. It can be observed that the selected parameters used for welding can create an appropriate weld profile. Few sputters can be seen in Figure 9; however, the overall quality of the joint is in satisfactory condition.

Using an SEM, the joint SEM picture with 115 × magnification is shown in Figure 10. The picture shown in Figure 10 is taken from the best sample with the average power of 240 W, frequency of 20 Hz, pulse time of 5.5 ms, and speed of 5.84 mm/s. As shown in Figure 10, the weld section is very smooth; in addition, there are no porosity, cracks or other weld defects. Moreover, the weight percentage of the elements for the weldment is detected at 7 points along the mid-section line, as presented in Figure 4. Variations in the weight percentages of elements along this line for the best sample are shown in Figure 11. As shown in Figure 11, the alloy composition on the left is Hastelloy X with the high nickel (about 44%) and low iron content (about 18%), and while moving to the right, the nickel content uniformly is reduced and the percentage of iron increases. The chromium weight percentage is

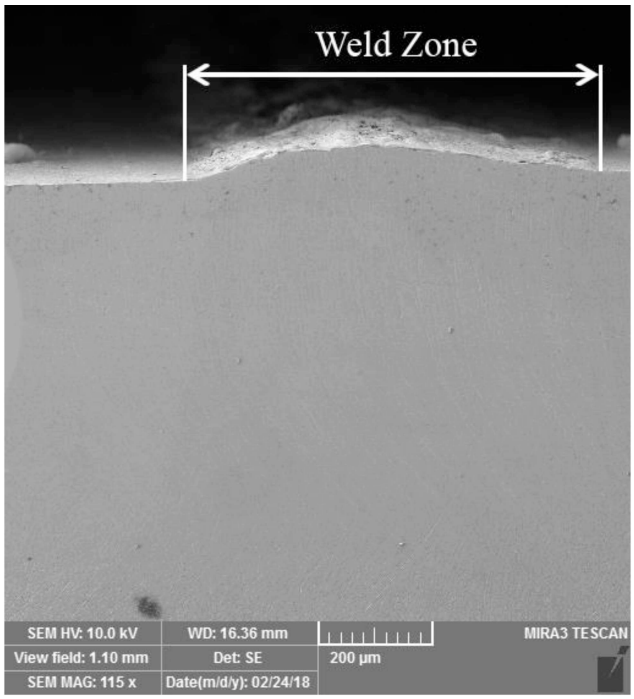

Figure 10. Scanning Electron Microscope (SEM) picture of weld section.

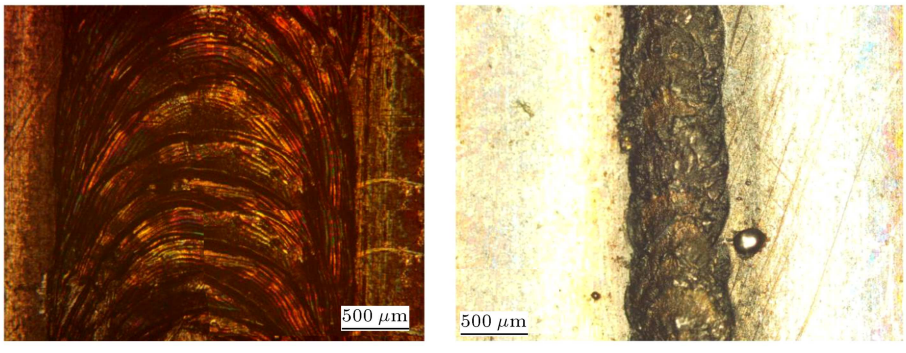

(a) (b)

Figure 9. Weld appearance for the best joint: (a) Top surface and (b) bottom surface.

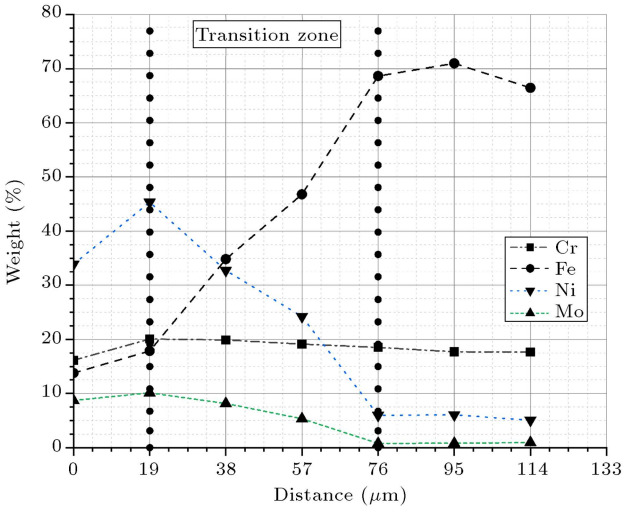

Figure 11. Changes in the weight percentage of the elements in the weld seam.

almost constant along this line. Furthermore, the Molybdenum content is reduced from about 10% at the start (Hastelloy X region) to about 0% (304L region). As observed in Figure 11, the width of the transition area is approximately 60 μm, and the regular change of elemental composition within this region reflects the satisfactory quality and mixture of the weldment.

5. Conclusion

The present study aimed to investigate the mechanical and material properties of dissimilar welding of Hastelloy X and AISI 304L using Nd-YAG pulsed laser beam. Two pieces of plates with the thickness of 1 mm were butt welded using a pulsed laser beam with different welding parameters. The mechanical strength of the joints was studied using a uniaxial tensile test machine at room temperature.

By means of optimizing the laser beam power and laser pulse width, the best welding parameters were selected. The results of the uniaxial tensile tests of the dissimilar joints and the base alloys showed that the excellent joints could be made between Hastelloy X and AISI 304L alloys. In this respect, the joint strength was calculated as 96% of the weaker base alloy strength (AISI 304L) at room temperature. In order to achieve the highest strength of the proposed welding, the proper welding parameters including laser power, welding speed, and pulse width should be 240 W, 5.84 mm/s, and 5.5 ms, respectively. The results also indicated that the average laser power and laser pulse width had maximum effect on the tensile joint strength. Furthermore, the pulse overlap percentage of more than 58% represents the maximum strength of joints.

The changes in the composition of the structural elements of the joint through the welding seam were investigated using a scan electron microscope. Moreover, the results of the scan electron microscope indicate that regarding the selected welding parameters, a relatively impressive mix of the elements was generated in the weld zone, and the changes in the percentage of the elements occurred regularly. Furthermore, the weld zone Scanning Electron Microscope (SEM) picture revealed that a sound joint could be achieved based on the selected parameters.

References

1. Mehta, K.K., Mukhopadhyay, P., Mandal, R.K., et al. "Mechanical properties anisotropy of cold-rolled and solution-annealed Ni-based Hastelloy C-276 alloy", *Metallurgical and Materials Transactions A*, **45**(8), pp. 3493–3504 (2014).

2. Kim, W.G., Yin, S.N., Ryu, W.S., et al. "Tension and creep design stresses of the Hastelloy-X alloy for high-temperature gas cooled reactors", *Materials Science and Engineering: A*, **483**, pp. 495–497 (2008).

3. Reddy, G.P., Harini, P., Sandhya, R., et al. "On dual-slope linear cyclic hardening of Hastelloy X", *Materials Science and Engineering: A*, **527**(16–17), pp. 3848–3851 (2010).

4. Vahidi, H. and Ghomsheie, M.M.A. "Comparison accurate calculate and numerical solution of buckling thin cylindrical shape memory alloy shell under uniform load with D.Q.M", *UCT Journal of Research in Science, Engineering and Technology*, **3**(3), pp. 33–38 (2015).

5. Pavan, A.H.V., Vikrant, K.S.N., Ravibharath, R., et al. "Development and evaluation of SUS 304H - IN 617 welds for advanced ultra supercritical boiler applications", *Materials Science and Engineering: A*, **642**, pp. 32–41 (2015).

6. Sharma, S., Taiwade, R.V., and Vashishtha, H. "Effect of continuous and pulsed current gas tungsten arc welding on dissimilar weldments between Hastelloy C-276/AISI 321 austenitic stainless steel", *Journal of Materials Engineering and Performance*, **26**(3), pp. 1146–1157 (2017).

7. Zhou, S., Chai, D., Yu, J., et al. "Microstructure characteristic and mechanical property of pulsed laser lap-welded nickel-based superalloy and stainless steel", *Journal of Manufacturing Processes*, **25**, pp. 220–226 (2017).

8. Kourdani, A. and Derakhshandeh-Haghighi, R. "Evaluating the properties of dissimilar metal welding between Inconel 625 and 316l stainless steel by applying different welding methods and consumables", *Metallurgical and Materials, Transactions A*, **49**(4), pp. 1231–1243 (2018).

9. Fabbro, R. "Developments in Nd:YAG laser welding", In Handbook of *Laser Welding Technologies*, S. Katayama, Ed., 1th Edn., pp. 47–72, Woodhead Publishing, Cambridge, UK (2013).

10. Zhan, X., Liu, Y., Ou, W., et al. "The numerical and experimental investigation of the multi-layer laser-MIG hybrid welding for Fe36Ni Invar alloy", *Journal of Materials Engineering and Performance*, **24**(12), pp. 4948–4957 (2015).
11. Kumar, P. and Sinha, A.N. "Microstructure and mechanical properties of pulsed Nd: YAG laser welding of st37 carbon steel", *Procedia Computer Science*, **133**, pp. 733–739 (2018).
12. Miller, K.J. and Nunnikhoven, J.D. "Laser-a space age welding process", *SAE Transactions*, pp. 485–493 (1966).
13. Myer, J.H. "Laser welding-a status report", No. 670211, SAE Technical Paper (1967).
14. Battista, A.D. and Ponti, M.A. "Laser welding of microcircuit interconnections-simultaneous multiple bonds of aluminum to kovar", No. 680802, SAE Technical Paper (1968).
15. Grajcar, A., Grzegorczyk, B., Róański, M., et al. "Microstructural aspects of bifocal laser welding of trip steels", *Archives of Metallurgy and Materials*, **62**(2), pp. 611–618 (2017).
16. Han, B., Tao, W., and Chen, Y. "New technique of skin embedded wire double-sided laser beam welding", *Optics & Laser Technology*, **91**, pp. 185–192 (2017).
17. Yang, J., Yu, Z., Li, Y., et al. "Laser welding/brazing of 5182 aluminium alloy to ZEK100 magnesium alloy using a nickel interlayer", *Science and Technology of Welding and Joining*, **23**(7), pp. 1–8 (2018).
18. Cai, X., Sun, D., Li, H., et al. "Dissimilar joining of TiAl alloy and Ni-based superalloy by laser welding technology using V/Cu composite interlayer", *Optics & Laser Technology*, **111**, pp. 205–213 (2019).
19. Mai, T.A. and Spowage, A.C. "Characterisation of dissimilar joints in laser welding of steel-kovar, copper-steel and copper-aluminium", *Materials Science and Engineering: A*, **374**(1–2), pp. 224–233 (2004).
20. Liu, X.B., Pang, M., Zhang, Z.G., et al. "Characteristics of deep penetration laser welding of dissimilar metal Ni-based cast superalloy K418 and alloy steel 42CrMo", *Optics and Lasers in Engineering*, **45**(9), pp. 929–934 (2007).
21. Liu, X.B., Yu, G., Pang, M., et al. "Dissimilar autogenous full penetration welding of superalloy K418 and 42CrMo steel by a high power CW Nd: YAG laser", *Applied Surface Science*, **253**(17), pp. 7281–7289 (2007).
22. Neves, M.D.M., Lotto, A., Berretta, J.R., Rossi, W., et al. "Microstructure development in Nd: YAG laser welding of AISI 304 and Inconel 600", *Welding International*, **24**(10), pp. 739–748 (2010).
23. Choobi, M.S., Haghpanahi, M., and Sedighi, M. "Investigation of the effect of clamping on residual stresses and distortions in butt-welded plates", *Scientia Iranica, Transactions B, Mechanical Engineering*, **17**(5), pp. 387–394 (2010).
24. Mortezaie, A. and Shamanian, M. "An assessment of microstructure, mechanical properties and corrosion resistance of dissimilar welds between Inconel 718 and 310S austenitic stainless steel", *International Journal of Pressure Vessels and Piping*, **116**, pp. 37–46 (2014).
25. Ates, H., Dursun, B., and Kurt, E. "Estimation of mechanical properties of welded S355J2+ N steel via the artificial neural network", *Scientia Iranica, Transactions B, Mechanical Engineering*, **23**(2), pp. 609–617 (2016).
26. Manikandan, M., Gunachandran, R., Vigneshwaran, M., et al. "Comparative studies on metallurgical and mechanical properties of bimetallic combination on incoloy 800 and ss 316L fabricated by gas metal and shield metal arc welding", *Transactions of the Indian Institute of Metals*, **70**(3), pp. 749–757 (2017).
27. Kumar, P. and Sinha, A.N. "Studies of temperature distribution for laser welding of dissimilar thin sheets through finite element method", *Journal of the Brazilian Society of Mechanical Sciences and Engineering*, **40**(9), p. 455 (2018).
28. Kumar, P. and Sinha, A.N. "Effect of pulse width in pulsed Nd:YAG dissimilar laser welding of austenitic stainless steel (304 L) and carbon steel (st37)", *Lasers in Manufacturing and Materials Processing*, **5**(4), pp. 317–334 (2018).
29. Davis, J.R., *Stainless Steels*, In ASM International Handbook Committee, 1th Edn. pp. 1–576, ASM International Press, Ohio, USA (1994).
30. Lippold, J.C., Kiser, S.D., and DuPont, J.N., *Welding Metallurgy and Weldability of Nickel-Base Alloys*, 1th Edn, pp. 1–456, John Wiley & Sons Press, New York City, USA (2011).

Biographies

Farid Vakili Tahami received his PhD in Mechanical Engineering from UMIST (Manchester University, England). He is currently an Associate Professor at the University of Tabriz, Department of Mechanical Engineering. His research interests are welding, mechanical design, and finite element modeling.

Ebrahim Safari received his PhD in the Laser Physics from Joseph Fourier University. He is currently an Associate Professor at the University of Tabriz, Department of Physics. His research interests are laser and laser welding.

Hamed Halimi Khosroshahi received his PhD in Mechanical Engineering from University of Tabriz. His research interests include finite element modeling, welding, laser cutting, and material design.